QuaRo: A Queue-Aware Robust Coordinated Transmission Strategy for Downlink C-RANs

Tuyen X. Tran, Abolfazl Hajisami, and Dario Pompili
Department of Electrical and Computer Engineering
Rutgers University–New Brunswick, NJ, USA
email: {tuyen.tran, hajisamik, pompili}@cac.rutgers.edu

***Abstract*—A queue-aware robust (QuaRo) coordinated transmission strategy is proposed for Cloud Radio Access Networks (C-RANs) with a central BaseBand processing Unit (BBU) connected to multiple Remote Radio Heads (RRHs). Such QuaRo strategy is adaptive to both user-traffic urgency via Queue State Information (QSI) and wireless channel opportunity via the observed (yet imperfect) Channel State Information (CSI). This involves clustering the RRHs into virtual user-centric clusters and performing Coordinated Beamforming (CB) from each virtual cluster to the target user in the downlink. The underlying control policy is formulated via Lyapunov optimization to minimize the average total transmit power at the RRHs while ensuring the stability of the system. In particular, the designed control policy does not require *a-priori* knowledge of the probability distribution of data-traffic arrival and channel states, and is robust against the instantaneous channel estimation error in each time slot. Extensive simulation results are presented to illustrate performance gains and robustness of the proposed solutions.**

***Index Terms*—Cloud Radio Access Networks; User-centric Clustering; Coordinated Beamforming; Lyapunov Optimization.**

I. Introduction

A. Overview

Over the last few years, the proliferation of personal mobile computing devices like tablets and smartphones along with a plethora of data-intensive mobile applications has resulted in a tremendous increase in demand for ubiquitous and high data-rate wireless communications. While the allocated bandwidth for each system is limited, current practice to enhance the spectral efficiency is to densify Base Station (BS) deployment in smaller cells and to increase the frequency reuse factor. However, additional deployment and maintenance of a large number of cellular BSs are highly inefficient due to excessive capital and operating expenditures. Moreover, in a fully-loaded cellular environment with a high frequency reuse factor, users at the cell boundaries are severely affected by the inevitable inter-cell interference [1]. To address such problem, Coordinated Multi-Point (CoMP) transmission and reception techniques [2] can be employed where neighboring BSs are grouped together to perform coordinated beamforming and/or joint processing. These techniques can help mitigate inter-cell interference and thus enhance the spectral efficiency at the cost, however, of higher-complexity receivers and overhead due to information exchange among the BSs. In current cellular-network architectures, physical links only exist between BSs and their corresponding access-network gateway; hence, the control signaling between BSs, which is needed to realize CoMP, has to travel through costly backhaul links, and often over a one-level higher layer in the aggregation hierarchy. Consequently, the latency and scarce interconnection capacity among BSs have resulted in limited deployments of CoMP in practice and, in turn, in modest BS cooperation.

Recently, Cloud Radio Access Network (C-RAN) [3], [4] has been introduced as a new paradigm for wireless cellular network that addresses the fluctuation in capacity demand efficiently while lowering the cost of delivering services to the users. Key characteristics of C-RAN include: i) centralized management of computing resources, ii) collaborative communications, and iii) real-time cloud computing on generic platforms. As shown in Fig. 1, a typical C-RAN is composed of multiple Remote Radio Heads (RRHs) distributed over a wide geographic region and a BaseBand processing Unit (BBU) consisting of general-purpose servers housed in a datacenter Cloud. The RRHs are connected to the BBU through high-bandwidth low-latency fronthaul links (e.g., optical fibers). Thanks to its centralized nature, C-RAN provides a higher degree of cooperation and communication among the BSs.

In this paper, we leverage the potential of C-RAN and design a queue-aware robust coordinated transmission strategy for downlink channels. Our proposed control policy aims at minimizing the average total transmit power at the RRHs while ensuring the stability of the queueing system at the BBU pool. The centralized model of the BBU allows for real-time inter-communication among the Virtual Base Station (VBS) deployed on the co-located servers, thus fully enabling dynamic reconfiguration of virtual user-centric RRH clusters and coordinated joint transmission of RRHs in each cluster. In this strategy, each virtual cluster is configured dynamically for a specific user by selecting the RRHs located in the vicinity of that user. This is different from traditional static and network-centric clustering approaches where the cluster boundaries are fixed and each RRH belongs to one cluster only. With a user-centric clustering of the RRHs, the problematic notion of cluster-edge is de-emphasized as each scheduled user is always a central of a cluster, which leads to lower inter-cluster interference and higher spectral efficiency.

B. Related Work

Pioneering works on realizing the benefit of C-RANs have focused on the overall system architecture with emphasis

978-1-5090-1732-4/16/$31.00 ©2016 IEEE

on system issues, feasibility of virtual software base station stacks, performance requirements, and analysis of optical links between RRHs and their VBSs [3], [5], [6].

On the other hand, advanced cooperation techniques for C-RAN have also been studied targeting different objectives. For example, the network power minimization problem is studied in [7], [8] using group-sparse beamforming techniques. The problem of weighted sum-rate maximization with user-centric clustering is studied in [9]–[11]. However, these works only focus on physical-layer performance of spectral efficiency or energy efficiency, and do not take into account the bursty arrival nature and latency requirement of delay-sensitive traffic. Therefore, the resulting control policy is only adaptive to the Channel State Information (CSI) and does not guarantee good delay performance for delay-sensitive applications.

Queue-aware dynamic resource allocation in stochastic wireless networks has been investigated in several works. For example, in [12], the authors proposed a delay-optimal dynamic clustering and power allocation for traditional multi-cell networks based on distributed stochastic learning; in [13], the authors proposed a queue-weighted dynamic optimization algorithm for the joint allocation of subframes, resource blocks, and power in relay-based LTE-A networks using a Lyapunov optimization approach. However, all these works assume that perfect CSI is available at the transmitter; consequently, such solution cannot work in C-RANs where practical challenges such as imperfect CSI at the BBU cannot be overlooked.

Unlike in these aforementioned works, in this paper we study a coordinated downlink transmission strategy that is adaptive to both channel and queue information in each scheduling slot. In addition, by considering the imperfect CSI available at the BBU pool, our solution is robust against channel estimation errors in practical systems.

C. Contributions

We propose a queue-aware robust coordinated downlink transmission strategy for C-RANs that is formulated according to the Lyapunov optimization theory so to minimize the average total transmit power at the RRHs while ensuring stability of the queueing system at the BBU cloud. The designed control policy does not require *a-priori* knowledge of the probability distribution of data-traffic arrival and channel states, and achieves throughput optimality given that the average arrival rates fall within the system stability region. In our proposed control policy, the BBU cloud observes both the Queue State Information (QSI) and (imperfect) CSI at the beginning of each scheduling slot, and makes decisions on the clustering of RRHs for each scheduled user together with the coordinated beamforming design of the RRHs in each cluster.

D. Paper Organization

The remainder of this paper is organized as follows: in Sect. II, we introduce the C-RAN system and present the considered channel and queuing models; in Sect. III, we describe the control policy design and formulate the per-slot optimization problem; in Sect. IV, we derive the user-centric clustering and queue-aware coordinated beamforming schemes. Then, in Sect. V, we illustrate the simulation results, and conclude the paper and point to future works in Sect. VI.

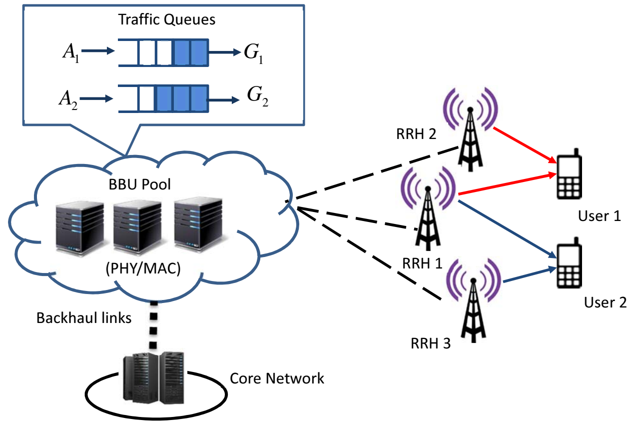

Fig. 1. Cloud Radio Access Network Architecture.

II. System Model

In this section, we introduce the considered C-RAN downlink system model, the physical-layer model with imperfect CSI consideration, and the bursty source model followed by queue dynamics and system stability definition.

A. C-RAN Downlink System

We consider a C-RAN system with multiple RRHs connected via high-capacity, low-latency fronthaul links to a BBU pool. We study the downlink transmission of the system in a single frequency band, which is considered to be spatially reused across all the users. Let $\mathcal{R} = \{1, 2, ..., R\}$ and $\mathcal{U} = \{1, 2, ..., U\}$ be the set of RRHs and active users in the system, respectively. For simplicity, we assume that each user has single antenna while each RRH is equipped with N antennae. It should be noted that our solution can be extended to the case of multi-antenna users and different number of antennae at the RRHs.

To take advantage of C-RAN in providing high orders of cooperation among the RRHs, we consider a user-centric coordinated downlink transmission strategy. In particular, based on the observed CSI in each scheduling slot, the central controller in the BBU pool adaptively forms a virtual cluster of RRHs for each scheduled user. In this scheme, each RRH can belong to multiple virtual clusters at the same time. The size of a cluster, defined as the number of RRHs in that cluster, can be flexibly chosen; however, the maximum cluster size might be constrained by different factors such as the maximum distance between RRHs in a cluster or the induced signaling overhead to realize cooperation strategy among the RRHs in a cluster.

Let $s_u^r(t)$ denote the association variable for user u and RRH r in tth scheduling slot, i.e., $s_u^r(t) = 1$ if RRH r is in the serving cluster of user u and $s_u^r(t) = 0$ otherwise. We also define $\mathcal{V}_u(t) = \{r \in \mathcal{R} \,|s_u^r(t) = 1\}$ as the serving cluster of user u in tth scheduling slot. Correspondingly, the set of users associated with RRH r in this slot is denoted as $\mathcal{U}(r,t) = \{u \in \mathcal{U} \,|s_u^r(t) = 1\}$. Note that each RRH can simultaneously serve at most N users, i.e., $|\mathcal{U}(r,t)| \le N, \forall r \in \mathcal{R}$.

B. Physical-layer Model

In the considered system, the scheduling is carried out in consecutive time slots indexed by $t \in \{1, 2, ...\}$, where t denotes the time interval $[t, t+\tau)$ and τ is the slot duration. In this paper, we refer to t as the time slot and scheduling slot interchangeably. In the tth slot, we denote $\mathbf{h}_u^r(t) \in \mathbb{C}^{1\times N}$ as the *actual* channel coefficient vector from RRH r to user u and $\mathbf{H}(t) = \{\mathbf{h}_u^r(t), u \in \mathcal{U}, r \in \mathcal{R}\}$ as the global CSI. It is assumed that $\mathbf{H}(t)$ is quasi static in each scheduling slot and is independent and identically distributed (i.i.d.) over different slots. In addition, $\mathbf{h}_u^r(t)$ is independent with respect to (w.r.t.) the slot index t and (u,r), $\forall u \in \mathcal{U}, r \in \mathcal{R}$.

We consider that perfect CSI is available at the users only while imperfect CSI at the Transmitter (CSIT) is obtained at the BBU pool. In practice, imperfect CSIT is usually achieved due to estimation errors and feedback latency in Frequency Division Duplex (FDD) systems or due to the duplexing delay in Time Division Duplex (TDD) systems. Let $\tilde{\mathbf{h}}_u^r(t) \in \mathbb{C}^{1\times N}$ be the imperfect estimation of $\mathbf{h}_u^r(t)$ available at the BBU pool and $\tilde{\mathbf{H}}(t) = \left\{\tilde{\mathbf{h}}_u^r(t), \forall u \in \mathcal{U}, r \in \mathcal{R}\right\}$ be the observed global CSIT. In this paper, we adopt a popular imperfect CSIT model as presented in [14], where $\tilde{\mathbf{h}}_u^r(t)$ is given as,

$$\tilde{\mathbf{h}}_u^r(t) = \mathbf{h}_u^r(t) + \sqrt{\epsilon_u}\mathbf{v}_u^r, \tag{1}$$

in which $\mathbf{v}_u^r \in \mathbb{C}^{1\times N}$ is a complex Gaussian random vector denoted as $\mathbf{v}_u^r \sim \mathcal{CN}(0, \mathbf{I}_N)$, and $\epsilon_u \in [0,1]$ is the CSIT error variance, which measures the CSIT quality and is assumed to be the same for all channel estimation from each user. In particular, when $\epsilon_u = 0$, we have $\tilde{\mathbf{h}}_u^r(t) = \mathbf{h}_u^r(t)$, which corresponds to the perfect CSIT case; and when $\epsilon_u = 1$, we have $\tilde{\mathbf{h}}_u^r(t)\left(\mathbf{h}_u^r(t)\right)^\dagger = 0$, which corresponds to the no CSIT case, where $(\cdot)^\dagger$ denotes the Hermitian operator.

During each scheduling slot, we assume that each user has a single traffic flow that is independent of all other users' flows. Users having multiple traffic flows is a special case of our considered system with multiple single-flow users at the same location. In the tth slot, let $x_u(t) \in \mathbb{C}$ denote the downlink data symbol of unit power for user u. It is assumed that $x_u(t)$ is independent from the receiver noise and time slot index t. The BBU pool processes baseband data signals for each user and computes the corresponding beamforming coefficients for the RRHs in the serving cluster of that user. In the tth slot, let $\mathbf{w}_u^r(t) \in \mathbb{C}^{N\times 1}$ be the linear downlink beamforming vector at RRH r for user u and $\mathbf{W}(t) = \{\mathbf{w}_u^r(t)\,|\forall u \in \mathcal{U}, r \in \mathcal{R}\}$ be the network beamforming design. Thus, the received signal $y_u(t) \in \mathbb{C}$ at user u is,

$$y_u(t) = \sum_{r\in\mathcal{V}_u} \mathbf{h}_u^r(t)\,\mathbf{w}_u^r(t)\,x_u(t) + z_u(t) + \underbrace{\sum_{u'\in\mathcal{U},u'\neq u}\sum_{r'\in\mathcal{V}_{u'}} \mathbf{h}_u^{r'}(t)\,\mathbf{w}_{u'}^{r'}(t)\,x_{u'}(t)}_{\text{interference}}, \tag{2}$$

where $z_u(t)$ is the zero-mean circularly symmetric Gaussian noise, denoted as $\mathcal{CN}(0,\sigma^2)$. The Signal-to-Interference-plus-Noise Ratio (SINR) at user u can be calculated as,

$$\gamma_u(t) = \frac{\left|\sum\limits_{r\in\mathcal{V}_u} \mathbf{h}_u^r(t)\,\mathbf{w}_u^r(t)\right|^2}{\sum\limits_{u'\in\mathcal{U},u'\neq u}\left|\sum\limits_{r'\in\mathcal{V}_{u'}} \mathbf{h}_u^{r'}(t)\,\mathbf{w}_{u'}^{r'}(t)\right|^2 + \sigma^2}. \tag{3}$$

With this position, the mutual information of user u in slot t can be calculated as $\Gamma_u(t) = \log_2(1+\gamma_u(t))$. Let $R_u(t)$ be the scheduled transmission rate $[\text{bit/s/Hz}]$ of user u in the tth slot, calculated using the observed CSIT $\tilde{\mathbf{H}}(t)$. Due to imperfect CSIT, there is uncertainty of the mutual information $\Gamma_u(t)$, which results in an outage probability associated with each scheduled transmission due to packet errors. Transmission outage occurs whenever the scheduled data rates exceeds the instantaneous mutual information despite the use of powerful error correction coding. Therefore, when the scheduled transmission rate is $R_u(t)$, the goodput [15] (i.e., the amount of data successfully delivered to user u) is,

$$G_u(t) = \begin{cases} R_u(t), & R_u(t) \le \Gamma_u(t), \\ 0, & \text{otherwise}. \end{cases} \tag{4}$$

C. Bursty Source Model

Let $A_u(t), u \in \mathcal{U}$, be the random data arrival rate $[\text{bits/s}]$ of user u (for downlink) in tth scheduling slot. It is assumed that the arrival process $A_u(t)$ is distributed according to a general distribution and is i.i.d. over scheduling slots and independent w.r.t. u. The average arrival rate for user u is denoted as $\lambda_u = \mathbb{E}[A_u(t)]$. Let $Q_u(t) \ge 0$ be the downlink queue length of user u, i.e., the number of bits in the queue maintained at the BBU pool for downlink data of user u, at the beginning of the tth scheduling slot. We denote as $\mathbf{Q}(t) = [Q_1(t), Q_2(t), ...Q_U(t)]$ the system QSI in the tth slot. The queue dynamic of user u evolves as follows [16],

$$Q_u(t+1) = [Q_u(t) - B\tau G_u(t)]^+ + A_u(t)\,\tau, \tag{5}$$

where B is the channel bandwidth, $[x]^+ = \max\{x, 0\}$, τ is the slot duration, and $G_u(t)$ is given in (4). In this paper, we assume that the packets arrived during each time slot are not observed when the control action of this slot is performed. Due to resource-allocation constraints, there are finite bounds on the second moment of the arrival rate and output rate (goodput) [17], defined as $A_{\max}^2 = \max\limits_u \sum\limits_{u\in\mathcal{U}} \mathbb{E}\left[A_u^2(t)\right]$ and $G_{\max}^2 = \max\limits_u \sum\limits_{u\in\mathcal{U}} \mathbb{E}\left[G_u^2(t)\right]$, respectively. Note that the queue dynamics of U users in the system are coupled together through the *interference* components, as shown in (2). In particular, the departure of the uth queue depends on the control actions of all the other data flows.

Following the definition in [16], we say that the queueing network of the system is *strongly stable* if

$$\lim_{T\to\infty}\sup\frac{1}{T}\sum_{t=1}^{T}\mathbb{E}[Q_u(t)] < \infty, \forall u \in \mathcal{U}. \tag{6}$$

The condition in (6) implies that a queue is strongly stable if it has a bounded time average backlog. Throughout the paper we will use the term 'stability' to refer to strong stability. Furthermore, the stability region $\mathcal{S}_\Omega$ of a control policy Ω is the set of average arrival rate vectors $\boldsymbol{\lambda} = \{\lambda_u \,| u \in \mathcal{U}\}$ for which the system is stable under Ω. Thus, the stability region of the system is $\bigcup_{\Omega \in \Psi} \mathcal{S}_\Omega$, where Ψ is the set of all feasible control policies satisfying the system stability condition. A *throughput-optimal* control policy is a policy that can stabilize the system for all arrival-rate vectors falling within the system stability region [16].

III. Problem Formulation

In this section we formulate the queue-aware robust coordinated downlink transmission policy, QuaRo, for the considered C-RAN system that aims at minimizing the average total transmit power at the RRHs while maintaining system stability. We use Lyapunov optimization theory to design a control policy that involves solving joint clustering and queue-aware coordinated beamforming problem in each scheduling slot.

A. Robust Coordinated Downlink Transmission Policy

Let Ω denote our proposed QuaRo downlink transmission policy that is adaptive to the system QSI and observed imperfect CSIT. In QuaRo, the decision process is formulated based on the system evolvement at discrete scheduling slots $\{t = 1, 2, ...\}$. At the beginning of each slot, the central controller in BBU pool observes the current $\tilde{\mathbf{H}}(t)$ and current $\mathbf{Q}(t)$, and makes a control action involving a clustering decision $\mathcal{V}(t)$ and a beamforming design $\mathcal{B}(t)$. We define the control policy Ω in each time slot t as follows,

$$\Omega\left(\tilde{\mathbf{H}}(t), \mathbf{Q}(t)\right) \triangleq (\mathcal{V}(t), \mathcal{B}(t)), \tag{7}$$

where $\mathcal{B}(t) = \{\mathbf{w}_u^r(t), \forall u \in \mathcal{U}, r \in \mathcal{R}\}$ and $\mathcal{V}(t) = \{s_u^r(t), \forall u \in \mathcal{U}, r \in \mathcal{R}\}$. In slot t, the transmit power at each RRH r calculated as,

$$P_r(t) = \sum_{u \in \mathcal{U}(r,t)} \|\mathbf{w}_u^r(t)\|_2^2, \forall r \in \mathcal{R}. \tag{8}$$

Thus, the total transmit power of all the RRHs is $P(t) = \sum_{r \in \mathcal{R}} P_r(t)$, and the time-average total transmit power of all the RRHs is,

$$\begin{aligned}\bar{P}(\Omega) &= \lim_{T\to\infty} \sup \frac{1}{T} \sum_{t=1}^{T} \mathbb{E}^\Omega [P(t)] \\ &= \lim_{T\to\infty} \sup \frac{1}{T} \sum_{t=1}^{T} \mathbb{E}^\Omega \left[\sum_{r\in\mathcal{R}} \sum_{u \in \mathcal{U}(r,t)} \|\mathbf{w}_u^r(t)\|_2^2\right].\end{aligned} \tag{9}$$

where $\mathbb{E}^\Omega[\cdot]$ denotes the expectation taken w.r.t. the measure induced by the given policy Ω.

In our proposed QuaRo policy, we aim at minimizing the time-average total transmission power cost while ensuring the queue stability condition in (6), i.e., the average service rate for each queue is greater than the average arrival rate. To realize this strategy, we formulate the underlying optimization problem as follows,

$$\begin{aligned}&\min_{\Omega} \sum_{u\in\mathcal{U}} \bar{P}(\Omega) \\ &\text{s.t.} \quad \lim_{T\to\infty} \sup \frac{1}{T} \sum_{t=1}^{T} \mathbb{E}^\Omega [Q_u(t)] < \infty, \forall u \in \mathcal{U}.\end{aligned} \tag{10}$$

Traditionally, this problem can be addressed using Dynamic Programming and Markov Decision Theory, which involve offline computations with very high complexity and require full *a-priori* knowledge of all system statistics [17]. Conversely, our approach employs Lyapunov optimization theory [18], [19], which caters to simple online decision making in each scheduling slot without requiring knowledge of the underlying probability distribution of data arrival and channel states.

B. Stochastic Lyapunov Optimization

An important and popular method to analyze the queue-aware resource control in wireless systems is to characterize the control policies in the stochastic stability sense using the *Lyapunov drift* theory [18], which is extended to the *Lyapunov optimization* theory [19]. We leverage Lyapunov optimization theory to stabilize the queuing system at the BBU pool while additionally minimizing the time-average total transmit power at the RRHs. In order to show the stability property of the queueing systems, we rely on the well-developed stability theory in Markov chains using the *negative Lyapunov drift*. In particular, the quadratic *Lyapunov function* for the system QSI at time slot t is defined as the sum of squares of the individual queue backlogs and is expressed as,

$$\mathcal{L}(\mathbf{Q}(t)) \triangleq \sum_{u\in\mathcal{U}} Q_u^2(t). \tag{11}$$

The *Lyapunov function* in (11) characterizes the extent of congestion in the queuing system. In particular, a small value of $\mathcal{L}(\mathbf{Q}(t))$ implies that all the queues are short, while a large value of $\mathcal{L}(\mathbf{Q}(t))$ means that at least one queue is long. Based on the *Lyapunov function*, we define the *one-step conditional Lyapunov drift* in slot t as,

$$\Delta(\mathbf{Q}(t)) \triangleq \mathbb{E}^\Omega [\mathcal{L}(\mathbf{Q}(t+1)) - \mathcal{L}(\mathbf{Q}(t)) | \mathbf{Q}(t)], \tag{12}$$

which represents the expected change in the *Lyapunov function* from one time slot to the next one under control policy Ω.

Let P^* represents the desired "target" average total transmit power expense at the RRHs; we now present the Lyapunov Optmization theorem w.r.t. the stochastic penalty process associated with the total transmit power $P(t)$ as follows.

Theorem 1. (Lyapunov Optimization) [19]: If there are positive constants V, η, Φ such that for all t and all $\mathbf{Q}(t)$, the Lyapunov drift satisfies,

$$\Delta(\mathbf{Q}(t)) + V\mathbb{E}[P(t) | \mathbf{Q}(t)] \le \Phi - \eta \sum_{u\in\mathcal{U}} Q_u(t) + VP^*, \tag{13}$$

then, we have

$$\lim_{T\to\infty} \sup \frac{1}{T}\sum_{t=1}^{T}\mathbb{E}\left[Q_u\left(t\right)\right] \leq \frac{\Phi + V\left(P^{*} - \overline{P}\right)}{\eta}, \tag{14}$$

and
$$\overline{P} \leq P^{*} + \Phi/V. \tag{15}$$

□

Thus, when Theorem 1 holds, the time-average total transmit power $\bar{P}$ is at most Φ/V beyond the target P^{*}. In other words, by adjusting the parameter V, $\bar{P}$ can be pushed arbitrarily close to the optimal value with a corresponding linear increase in the upper bound of the time-average queue length on the left hand side of (14). Theorem 1 suggests that the optimal control policy Ω is achieved by greedily minimizing the *Lyapunov-drift-plus-penalty function* on the LHS of (13) in each time slot, i.e., by minimizing,

$$\Delta\left(\mathbf{Q}\left(t\right)\right) + V\mathbb{E}^{\Omega}\left[P\left(t\right)\middle|\,\mathbf{Q}\left(t\right)\right], \tag{16}$$

where the expectation is taken over all possible control actions $\{\mathcal{V}\left(t\right), \mathcal{B}\left(t\right)\}$. Such a control policy Ω can achieve the power-delay tradeoff of $[\mathcal{O}\left(1/V\right), \mathcal{O}\left(V\right)]$ by adjusting the parameter V (refer to [16] for the proof). We have the following Lemma.

Lemma 1. A control policy that minimizes the time-average total transmit power while ensuring queue stability can be obtained by solving the *per-slot* optimization problem below,

$$\max_{\Omega=\{\mathcal{V}(t),\mathcal{B}(t)\}} \sum_{u\in\mathcal{U}} Q_u\left(t\right)G_u\left(t\right) - VP\left(t\right), \forall t. \tag{17}$$

Proof. See Appendix A. □

For simplicity, we will drop the time index t in subsequent analyses and express the problem in (17) as a *per-slot* queue-aware clustering and coordinated beamforming problem below,

$$\max_{\{\mathcal{V},\mathcal{B}\}} \sum_{u\in\mathcal{U}} Q_uG_u - VP. \tag{18}$$

IV. Queue-aware Clustering and Coordinated Beamforming (QCB)

We derive here the solution to the queue-aware clustering and coordinated beamforming problem presented in (18). Firstly, to achieve a low-complexity solution, the clustering decision is determined via a simple heuristic algorithm that selects the RRHs around each user to form virtual clusters. Given a clustering decision, we then focus on the Queue-aware Coordinated Beamforming (QCB) problem, which is non-convex and contains an outage probability constraint that does not have a closed-form expression. To overcome these difficulties, we apply a *Bernstein-type* inequality to derive a closed-form approximation of the outage probability constraint. The QCB problem is then effectively solved using a novel proposed iterative algorithm based on a SemiDefinite Relaxation (SDR) approach.

A. Heuristic User-centric Clustering

A clustering decision specifies the association between users and RRHs. Generally, in a network with U users and R RRHs, the optimal clustering decision can be found via exhaustive search over 2^{UR} possible clustering patterns. Apparently this is not a practical approach given the large number of association variables s_u^r's. Hence, in this paper, we aim for a low-complexity clustering decision that can be made in each time slot based on the received signal strength from the surrounding RRHs at each scheduled user.

We consider that each virtual cluster has K RRHs, i.e., $K = \left|\mathcal{V}_u\right|, \forall u \in \mathcal{U}$. Based on the observed imperfect CSI at the BBU pool, the central controller forms a serving cluster for each user u by selecting K RRHs having the strongest channel gains, $\left|\tilde{\mathbf{h}}_u^r\right|$, to user u. It is assumed that an admission control process is performed prior to the clustering decision to ensure that the number of users associated to each RRH does not exceed N (the number of transmit antennae on each RRH). While admission control is out of the scope of this paper, it is worth noting that a simple greedy user-selection algorithm can be employed (see, for example, [20]).

It is reasonable to argue that the use of imperfect CSIT for heuristic clustering is relatively good because: i) in practice, the CSIT error in the C-RAN downlink systems cannot be too large, otherwise multi-user interference will severely limit the system performance of spatial multiplexing [21]; and ii) the dominating factor for clustering is the long-term path-loss and shadowing, as studied in [22].

B. Queue-aware Coordinated Beamforming

Given the clustering decision determined by the heuristic algorithm described in the previous section, we now consider the QCB design problem. In particular, for a given $\mathcal{V}$, we need to find the optimal beamforming design $\mathcal{B}^{*}$ by solving the QCB problem below,

$$\max_{\substack{\mathbf{w}_u^r\\ u\in\mathcal{U},r\in\mathcal{R}}} \sum_{u\in\mathcal{U}} Q_uG_u - V\sum_{r\in\mathcal{R}}\sum_{u\in\mathcal{U}(r)} \|\mathbf{w}_u^r\|_2^2. \tag{19}$$

Let ρ_u be the target outage probability corresponding to the delivery of data signals to user u given the observed system state $\left(\tilde{\mathbf{H}}, \mathbf{Q}\right)$, i.e.,

$$\Pr\left[R_u \leq \Gamma_u \middle|\tilde{\mathbf{H}}, \mathbf{Q}\right] \geq 1 - \rho_u, \forall u \in \mathcal{U}. \tag{20}$$

From (4) and (20), we recast the QCB problem in (19) as,

$$\max_{\substack{\mathbf{w}_u^r, R_u,\\ u\in\mathcal{U},r\in\mathcal{R}}} \sum_{u\in\mathcal{U}} Q_uR_u\left(1-\rho_u\right) - V\sum_{r\in\mathcal{R}}\sum_{u\in\mathcal{U}(r)} \|\mathbf{w}_u^r\|_2^2, \tag{21a}$$

$$\text{s.t.} \quad \Pr\left[R_u \leq \Gamma_u \middle|\tilde{\mathbf{H}}, \mathbf{Q}\right] \geq 1 - \rho_u, \forall u \in \mathcal{U}, \tag{21b}$$

$$0 \leq \rho_u \leq 1, \forall u \in \mathcal{U}. \tag{21c}$$

Note that the optimization variables are now the beamforming vectors $\{\mathbf{w}_u^r\}$ and the scheduled transmission rates $\{R_u\}$. Problem (21) is very difficult to solve as it is non-convex and the conditional probability constraint in (21b) does not have a closed-form expression. To overcome these drawbacks, our approach is to use a *Bernstein-Type Inequality* to derive a closed-form approximation of such constraint. Finally, the QCB problem is solved by a novel iterative algorithm based on a SDR approach.

For convenience, let $\mathbf{w}_u = vec\left(\mathbf{w}_u^r, r \in \mathcal{V}_u\right) \in \mathbb{C}^{NK\times 1}$ be the beamforming vector to user u from its serving cluster, where the $vec\left(\cdot\right)$ operator stacks all elements of $\mathbf{w}_u^r$'s, $r \in \mathcal{V}_u$, into a long column-vector. Similarly, let $\mathbf{h}_u = vec\Big(\left(\mathbf{h}_u^r\right)^T, \forall r \in \mathcal{V}_u\Big)^T \in \mathbb{C}^{1\times NK}$ and $\mathbf{h}_{u,u'} = vec\Big(\Big(\mathbf{h}_u^{r'}\Big)^T, \forall r' \in \mathcal{V}_{u'}, u' \neq u\Big)^T \in \mathbb{C}^{1\times NK}$.

From (3), we rewrite the mutual information expression as,

$$\Gamma_u = \log_2\left(1 + \frac{\left|\mathbf{h}_u\mathbf{w}_u\right|^2}{\sum\limits_{u'\in\mathcal{U}, u'\neq u}\left|\mathbf{h}_{u,u'}\mathbf{w}_{u'}\right|^2 + \sigma^2}\right), \forall u \in \mathcal{U}. \tag{22}$$

Now, by substituting the imperfect CSIT expression from (1) into (22) and performing some algebraic manipulations, it can be shown that constraint (21b) is equivalent to

$$\Pr\left[J_u\mathbf{K}_u(J_u)^\dagger + 2\mathrm{Re}\left\{J_uY_u\right\} \geq \beta_u\right] \geq 1 - \rho_u, \forall u \in \mathcal{U}, \tag{23}$$

where

$$\mathbf{K}_u = \epsilon_u\left(\mathbf{w}_u\mathbf{w}_u^\dagger - \tilde{\gamma}_u\sum_{u'\in\mathcal{U}, u'\neq u}\mathbf{w}_{u'}\mathbf{w}_{u'}^\dagger\right), \tag{24a}$$

$$Y_u = \sqrt{\epsilon_u}\left(\mathbf{w}_u\mathbf{w}_u^\dagger\tilde{\mathbf{h}}_u^\dagger - \tilde{\gamma}_u\sum_{u'\in\mathcal{U}, u'\neq u}\mathbf{w}_{u'}\mathbf{w}_{u'}^\dagger\tilde{\mathbf{h}}_{u,u'}^\dagger\right), \tag{24b}$$

$$\beta_u = \sigma^2 - \left|\tilde{\mathbf{h}}_u\mathbf{w}_u\right|^2 - \tilde{\gamma}_u\sum_{u'\in\mathcal{U}, u'\neq u}\left|\tilde{\mathbf{h}}_{u,u'}\mathbf{w}_{u'}\right|^2, \tag{24c}$$

$$\text{and} \quad \tilde{\gamma}_u = 2^{R_u} - 1, \quad J_u = vec\Big(\left(\mathbf{v}_u^r\right)^T, r \in \mathcal{V}_u\Big)^T. \tag{25}$$

The probability inequality in (23) contains a quadratic form of complex Gaussian random variables. We will now derive a closed-form approximation of (23) based on a Bernstein-type inequality using the following lemma.

Lemma 2. (Bernstein-Type Inequality [23]): Let $C = J\mathbf{K}J^\dagger + 2\mathrm{Re}\left\{JY\right\}$, where $\mathbf{K} \in \mathbb{H}^{NK\times NK}$ is a complex Hermitian matrix, $Y \in \mathbb{C}^{NK\times 1}$, and $J \sim \mathcal{CN}\left(0, \mathbf{I}_{NK\times NK}\right)$. Then, for any $\delta > 0$, we have,

$$\Pr\left[C \geq \mathrm{Tr}\left(\mathbf{K}\right) - \sqrt{2\delta}\sqrt{\|\mathbf{K}\|_F^2 + 2\|Y\|^2} - \delta(\lambda_{\max}\left(-\mathbf{K}\right))^+\right] \geq 1 - e^{-\delta}, \tag{26}$$

where $\lambda_{\max}\left(-\mathbf{K}\right)$ denotes the maximum eigenvalue of matrix $-\mathbf{K}$ and $\|\cdot\|_F$ represents the matrix Frobenius norm. □

The inequality in (26) bounds the probability that the quadratic form C of complex Gaussian random variables deviates from its mean $\mathrm{Tr}(\mathbf{K})$. Based on Lemma 2 and by setting $\delta_u = -\ln\left(\rho_u\right)$, we can obtain a conservative form of the conditional probability constraint in (23) as follows,

$$\mathrm{Tr}\left(\mathbf{K}_u\right) - \sqrt{2\delta_u}\sqrt{\|\mathbf{K}_u\|_F^2 + 2\|Y_u\|^2} - \delta_u(\lambda_{\max}\left(-\mathbf{K}_u\right))^+ \geq \beta_u. \tag{27}$$

In other words, (27) is a sufficient condition for the conditional probability constraint in (23).

Given the closed-form approximation in (27), and by introducing the slack variables $\xi_u, \phi_u \in \mathbb{R}$, we have the conservative formulation of the QCB problem (21) as follows,

$$\min_{\substack{\mathbf{w}_u, \tilde{\gamma}_u, \xi_u, \phi_u \\ u\in\mathcal{U}}} \sum_{u\in\mathcal{U}} Q_u\big(e^{-\delta_u} - 1\big)\log_2\left(1 + \tilde{\gamma}_u\right) + V\sum_{u\in\mathcal{U}}\|\mathbf{w}_u\|_2^2 \tag{28a}$$

$$\text{s.t.} \quad \mathrm{Tr}\left(\mathbf{K}_u\right) - \sqrt{2\delta_u}\xi_u - \delta_u\phi_u \geq \beta_u, \forall u \in \mathcal{U}, \tag{28b}$$

$$\sqrt{\|\mathbf{K}_u\|_F^2 + 2\|Y_u\|^2} \leq \xi_u, \forall u \in \mathcal{U}, \tag{28c}$$

$$\phi_u\mathbf{I}_{NK\times NK} + \mathbf{K}_u \succeq 0, \forall u \in \mathcal{U}, \tag{28d}$$

$$\phi_u \geq 0, \delta_u \geq 0, \forall u \in \mathcal{U}. \tag{28e}$$

The problem in (28) is still non-convex since $\mathbf{K}_u$, Y_u, and β_u are indefinite quadratic w.r.t. $\{\mathbf{w}_u\}$. In order to convexify it, we use the SDR technique in [24]. Let us define $\mathbf{W}_u = \mathbf{w}_u(\mathbf{w}_u)^\dagger$. We can verify that $\mathbf{W}_u \succeq 0$ and $\mathrm{rank}\left(\mathbf{W}_u\right) = 1$. By temporarily removing the rank-one constraint on $\mathbf{W}_u$, we have the equivalent SDR form of (28) as follows,

$$\min_{\substack{\mathbf{W}_u, \tilde{\gamma}_u, \xi_u, \phi_u \\ u\in\mathcal{U}}} \sum_{u\in\mathcal{U}} Q_u\left(e^{-\delta_u} - 1\right)\log_2\left(1 + \tilde{\gamma}_u\right) + V\sum_{u\in\mathcal{U}}\mathrm{Tr}\left(\mathbf{W}_u\right) \tag{29a}$$

$$\text{s.t.} \quad \mathrm{Tr}\left(\mathbf{K}_u\left(\mathbf{W}\right)\right) - \sqrt{2\delta_u}\xi_u - \delta_u\phi_u \geq \beta_u\left(\mathbf{W}\right), \forall u \in \mathcal{U}, \tag{29b}$$

$$\sqrt{\|\mathbf{K}_u\left(\mathbf{W}\right)\|_F^2 + 2\|Y_u\left(\mathbf{W}\right)\|^2} \leq \xi_u, \forall u \in \mathcal{U}, \tag{29c}$$

$$\phi_u\mathbf{I}_{NK\times NK} + \mathbf{K}_u\left(\mathbf{W}\right) \succeq 0, \forall u \in \mathcal{U}, \tag{29d}$$

$$\phi_u \geq 0, \delta_u \geq 0, \mathbf{W}_u \succeq 0, \forall u \in \mathcal{U}, \tag{29e}$$

where $\mathbf{W} \triangleq \{\mathbf{W}_u : \forall u \in \mathcal{U}\}$, $\mathbf{K}_u\left(\mathbf{W}\right)$, $Y_u\left(\mathbf{W}\right)$, and $\beta_u\left(\mathbf{W}\right)$ are obtained by substituting $\mathbf{w}_u(\mathbf{w}_u)^\dagger$ by $\mathbf{W}_u$ into (24a), (24b), and (24c), respectively.

Note that the objective function in (29a), the second-order cone constraint in (29c), the positive semidefinite constraint in (29d), and the linear constraints in (29e) are all convex w.r.t. $\{\mathbf{W}_u, \tilde{\gamma}_u, \xi_u, \phi_u\}$. Furthermore, the constraint in (29b) is equivalent to $f_u\left(\mathbf{W}_u, \tilde{\gamma}_u, \xi_u, \phi_u\right) = \beta_u\left(\mathbf{W}\right) - \mathrm{Tr}\left(\mathbf{K}_u\left(\mathbf{W}\right)\right) + \sqrt{2\delta_u}\xi_u + \delta_u\phi_u \leq 0, \forall u \in \mathcal{U}$. It can be verified that the Hessian matrix of $f_u\left(\mathbf{W}_u, \tilde{\gamma}_u, \xi_u, \phi_u\right)$ is positive semidefinite, thus it is a convex function. In summary, (29) is a convex optimization problem.

Let us define $\tilde{\boldsymbol{\gamma}} = [\tilde{\gamma}_1, \tilde{\gamma}_2, ...\tilde{\gamma}_U]$. In the following, we propose an iterative SemiDefinite Programming (SDP) algorithm to solve problem (29). At each iteration, we temporarily fix the value of $\tilde{\gamma}$ and solve an SDP problem to obtain the optimal values $\mathbf{W}_u^*, \xi_u^*$ and ϕ_u^*. The value of $\tilde{\gamma}$ is updated in the next iteration using the subgradient method in [25]. In particular, for a given $\tilde{\gamma}$, we define the optimal-value function $\Lambda(\tilde{\gamma})$ as,

$$\Lambda(\tilde{\gamma}) = \sum_{u\in\mathcal{U}} Q_u\left(e^{-\delta_u}-1\right)\log_2\left(1+\tilde{\gamma}_u\right) + V\sum_{u\in\mathcal{U}} \mathrm{Tr}\left(\mathbf{W}_u^*\right), \tag{30}$$

where $\mathbf{W}_u^*$ is the optimal solution of (29) given a fixed $\tilde{\gamma}$. We summarize the iterative SDP algorithm in Algorithm 1 below.

Algorithm 1 Iterative SDP Algorithm

(1) Initialization: Set $n := 0$, and set $\tilde{\gamma}(0) = [\tilde{\gamma}_1(0), \tilde{\gamma}_2(0), \ldots\tilde{\gamma}_U(0)] > 0$.

(2) Given $\tilde{\gamma}(n)$, solve the following SDP problem using interior-point method [26] to obtain the optimal solution $\{\mathbf{W}_u^*(n), \xi_u^*(n), \phi_u^*(n)\}$.

$$\min_{\substack{\mathbf{W}_u,\xi_u,\phi_u \\ u\in\mathcal{U}}} \sum_{u\in\mathcal{U}} \mathrm{Tr}\left(\mathbf{W}_u\right) \tag{31a}$$

$$\text{s.t.} \quad (29b), (29c), (29d), (29e). \tag{31b}$$

(3) Calculate $\tilde{\gamma}(n+1)$ following the subgradient method as follows,

$$\tilde{\gamma}(n+1) = \tilde{\gamma}(n) - \alpha_n \mathbf{g}(n), \tag{32}$$

where $\mathbf{g}(n) = [g_1(n), \ldots g_U(n)]$ is a subgradient of $\Lambda(\tilde{\gamma})$ at $\tilde{\gamma}(n)$ and $\alpha_n > 0$ is the nth step size satisfying

$$\lim_{n\to\infty} \alpha_n = 0, \qquad \sum_{n=1}^{\infty} \alpha_n = \infty. \tag{33}$$

(4) Termination: Set $n := n+1$ and repeat Step (2) and (3) until convergence.

If we obtain $\mathbf{W}_u^*$ of rank one, it can be decomposed as $\mathbf{W}_u^* = \mathbf{w}_u^*(\mathbf{w}_u^*)^\dagger$ and thus $\mathbf{w}_u^*$ is the optimal solution of (28). Otherwise, we can apply standard rank-reduction techniques such as the Gaussian Randomization Procedure [24] to obtain a rank-one approximation of $\mathbf{W}_u^*$.

In Algorithm 1, the optimal solution $\mathbf{W}_u^*$ minimizes the objective function of (29) in each iteration. The optimal-value function $\Lambda(\tilde{\gamma})$ is the point-wise minimum of the objective function of (29), thus it is a convex function w.r.t. $\tilde{\gamma}$ [26]. Therefore, by using the diminishing step size α_n as in (33), the iterative algorithm will converge to an optimal solution [25].

The overall complexity of our QuaRo strategy comes from the optimization of the the per-slot QCB problem, which is solved by Algorithm 1. In can be seen that the complexity of this algorithm mainly comes from solving the SDP problem in (31), which is polynomial in problem size and number of constraints [26], i.e., polynomial w.r.t U, R, and N.

V. Performance Evaluation

In this section, simulation results are presented to illustrate the performance gain of our proposed QuaRo strategy. We consider a C-RAN system consisting of 16 wrap-around hexagonal cells with 1 Km inter-cell spacing. Each RRH is placed in the center of a cell and is equipped with $N = 4$ antennae. The wireless channels in the system are assumed to be *quasi-static* such that the channel coefficients stay constant during each scheduling slot but vary independently from one slot to another. The channel coefficients are calculated following the path-loss model, given as $L[\text{dB}] = 15.1 + 37.5\log_{10}(d[\text{m}])$, with the fading coefficient distributed as $\mathcal{CN}(0,1)$.

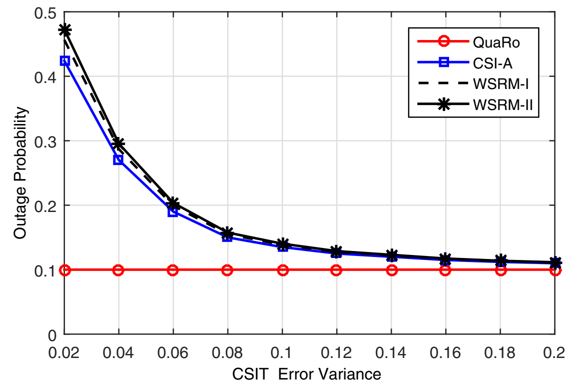

Fig. 2. Outage probability versus CSIR error variance with scheduled rate $R_u = 1$ bit/s/Hz, $\forall u$.

We use Poisson packet arrival with average rate λ_u [packets/slot] and deterministic packet size $N_u = 10$ Kbits, $\forall u$. The duration of each scheduling slot is $\tau = 5$ ms. The noise spectral density is -100 dBm/Hz and the channel bandwidth is $B = 10$ MHz, which is reused across all the users. For each simulation, we perform 300 drops in which 32 single-antenna users are placed randomly in the network.

The performance of our QuaRo strategy is compared with that of a *CSI-Adaptive* (CSI-A) and two popular *weighted sum-rate maximization* (WSRM) schemes, as described below.

- *CSI-A*: This scheme is a derivation of QuaRo strategy, but is only adaptive to the CSI. Specifically, we substitute the objective function in problem (29) by $\sum_{u\in\mathcal{U}}\left(\left(e^{-\delta_u}-1\right)\log_2\left(1+\tilde{\gamma}_u\right) + V\mathrm{Tr}\left(\mathbf{W}_u\right)\right)$, where V controls the tradeoff between the total transmit power and the sum output rates.
- *WSRM-I*: A downlink joint clustering and beamforming scheme proposed in [22], where the clustering algorithm is the same as of QuaRo and the clustered virtual SINR (CVSINR) algorithm is for beamforming design.
- *WSRM-II*: A greedy clustering algorithm proposed in [27], which solves an equivalent set covering problem to select the set of non-overlapping base station clusters. This scheme uses Zero-Forcing (ZF) beamforming.

Both WSRM-I and WSRM-II aim at maximizing the downlink weighted sum-rate where the weight of each flow is inverse proportional to the long-term average throughput.

Outage performance: In Fig. 2, we compare the average outage probabilities of the four competing schemes at different values of the CSIT error variance ϵ when the scheduled rates

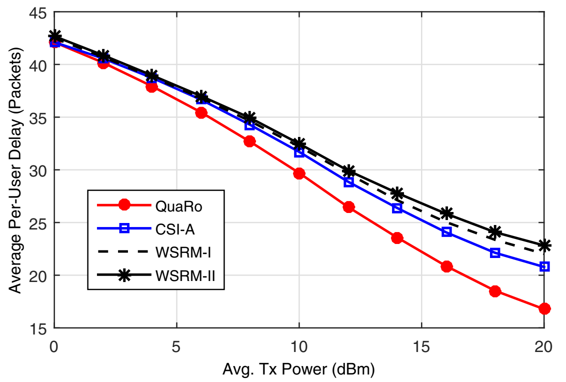

Fig. 3. Average per-user delay versus average per-RRH transmit power with $\epsilon = 0.1$, $\rho_u = 0.1$ and $\lambda_u = 5$ packets/slot, $\forall u$.

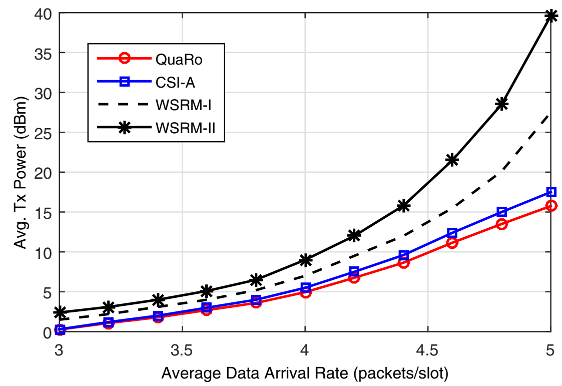

Fig. 4. Average per-RRH transmit power versus average data arrival rate with $\epsilon = 0.1$, $\rho_u = 0.1, \forall u$ and average per-user delay being 20 packets.

is $R_u = 1$ bit/s/Hz, $\forall u$. For each value of ϵ, we control the average total transmit power of the four schemes to be the same, but vary it so as to maintain the target outage probability $\rho_u = 0.1, \forall u, \epsilon$ for QuaRo scheme. We observe that, when spending the same average transmit power and scheduling the same output rate, the three baseline schemes always have higher outage probabilities than that of our QuaRo scheme, especially when ϵ is small. When ϵ increases, the outage performance of all schemes get closer. In fact, it is not practical to operate a system with large channel estimation error since we have to spend a very high amount of transmit power to maintain a low outage probability.

Delay-power trade-off: In Fig. 3, we plot the tradeoff between average per-user delay and average per-RRH transmit power. The average delays of all the schemes decrease as the average transmit power increases. In QuaRo and CSI-A schemes, each point on the delay-power trade-off curve corresponds to a different value of the control parameter V. It can be seen that our proposed QuaRo strategy achieves the best trade-off performance and that the gains—which come from the QSI-aware clustering and beamforming control—become more significant in high SNR regimes.

Transmit power versus arrival rate: The total average transmit power at the RRHs is illustrated in Fig. 4 versus different average data arrival rates. We observe that the power costs of the baseline schemes are always higher than that of QuaRo scheme. These gaps are more significant at large values of average data-arrival rates.

Impact of cluster size: In Figs. 5(a-b), we evaluate the impact of cluster size K (number of RRHs on each cluster) on the performance of our proposed QuaRo strategy. We consider two user distribution scenarios where 32 users are placed randomly in 16 cells: (a) *Uniform*—each cell has 2 users, and (b) *Non-uniform*—we randomly choose 8 heavy (loaded) cells, each having 3 users and 8 light cells, each having 1 user. The average per-RRH transmission power is plotted versus different cluster sizes with 95% confidence interval so to obtain statistical relevance of the results. It can be seen that the performance of QuaRo is improved when

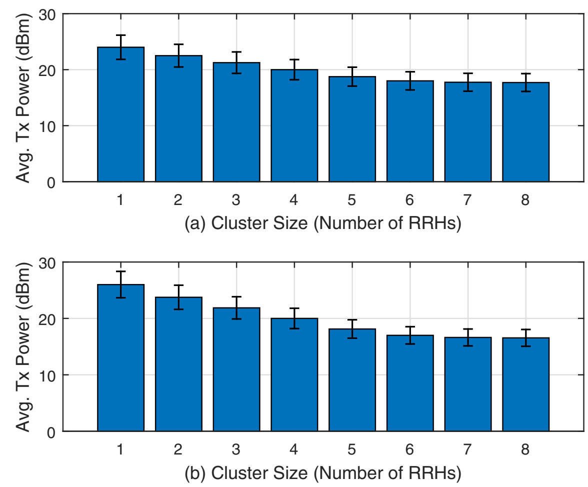

Fig. 5. Average Per-RRH Transmit Power versus Cluster Size with $\epsilon = 0.1$, $\rho_u = 0.1, \forall u$ and average per-user delay being 20 packets; (a) Uniform user distribution and (b) Non-uniform user distribution.

the cluster sizes are increased, in the sense that it requires lower total average transmit power at the RRHs to maintain the same average per-user delay, for the same values of ϵ, ρ_u. The improvement is more significant in the *non-uniform* user distributed scenario where the users in heavy cells benefit more from RRH cooperation. In both cases, we observe in our simulations that the the gains are negligible when $K \geq 6$.

VI. Conclusions

We have presented a queue-aware robust coordinated downlink transmission control policy for C-RANs. Our proposed QuaRo strategy optimizes the time-average power-delay trade-off by performing user-centric clustering and coordinated beamforming in each scheduling slot. Both Queue State Information (QSI) and imperfect Channel State Information at the Transmitter (CSIT) are taken into account in the algorithm design of QuaRo. Simulation results have demonstrated the significant performance gains and robustness of our proposed control policy over traditional approaches.

Future Works: It is worth investigating the channel estimation overhead and error variance associated with different cluster sizes in our scheme. We also plan to evaluate the real-world performance and feasibility of QuaRo strategy in our existing small-scale C-RAN testbed. In particular, we have implemented a testbed using an open-source LTE platform running on a general-purpose desktop server, connected to a set of RRHs implemented on USRP B210s.

APPENDIX A

The Lyapunov drift expression in (12) is rewritten as,

$$\Delta\left(\mathbf{Q}\left(t\right)\right) = \mathbb{E}^{\Omega}\left[\sum_{u\in\mathcal{U}}\left(Q_u^2\left(t+1\right) - Q_u^2\left(t\right)\right)\Big|\,\mathbf{Q}\left(t\right)\right]. \quad (34)$$

By squaring both sides of (5) and following the fact that $\left([x]^+\right)^2 \leq x^2$, we get

$$Q_u^2\left(t+1\right) \leq \left[Q_u\left(t\right) - B\tau G_u\left(t\right)\right]^2 + A_u^2\left(t\right)\tau^2 + 2A_u\left(t\right)\tau\left[Q_u\left(t\right) - B\tau G_u\left(t\right)\right]^+. \quad (35)$$

Since $\left[Q_u\left(t\right) - B\tau G_u\left(t\right)\right]^+ \leq Q_u\left(t\right)$, (35) leads to

$$Q_u^2\left(t+1\right) - Q_u^2\left(t\right) \leq B^2\tau^2G_u^2\left(t\right) + A_u^2\left(t\right)\tau^2 - 2Q_u\left(t\right)\left(B\tau G_u\left(t\right) - A_u\left(t\right)\tau\right). \quad (36)$$

By summing over all u's and taking conditional expectation on both sides of (36), we obtain

$$\begin{aligned}\Delta\left(\mathbf{Q}\left(t\right)\right) &\leq \sum_{u\in\mathcal{U}}\mathbb{E}\left[B^2\tau^2G_u^2\left(t\right) + A_u^2\left(t\right)\tau^2\big|\,\mathbf{Q}\left(t\right)\right] \\ &\quad - 2\sum_{u\in\mathcal{U}}\left(\mathbb{E}\left[Q_u\left(t\right)B\tau G_u\left(t\right)\big|\,\mathbf{Q}\left(t\right)\right] - \lambda_u\left(t\right)\tau\right) \\ &\leq U\tau^2\left(B^2G_{\max}^2 + A_{\max}^2\right) \\ &\quad - 2\sum_{u\in\mathcal{U}}\left(\mathbb{E}\left[Q_u\left(t\right)B\tau G_u\left(t\right)\big|\,\mathbf{Q}\left(t\right)\right] - \lambda_u\left(t\right)\tau\right). \quad (37)\end{aligned}$$

By letting $\Phi = U\tau^2\left(B^2G_{\max}^2 + A_{\max}^2\right)$ and adding the same value to both side of the inequality in (37), we get

$$\begin{aligned}\Delta\left(\mathbf{Q}\left(t\right)\right) + V\mathbb{E}\left[P\left(t\right)|\mathbf{Q}\left(t\right)\right] &\leq \Phi + 2\tau\sum_{u\in\mathcal{U}}\lambda_u\left(t\right) \\ &\quad - \mathbb{E}\left[2\tau B\sum_{u\in\mathcal{U}}Q_u\left(t\right)G_u\left(t\right) - VP\left(t\right)\big|\,\mathbf{Q}\left(t\right)\right]. \quad (38)\end{aligned}$$

With this position, we can follow the Energy-Efficient Control Algorithm (EECA) in [16], which is designed to maximize the second term on the Right Hand Side (RHS) of (38). It is shown that EECA guarantees queue stability while achieving $\left[\mathcal{O}\left(1/V\right), \mathcal{O}\left(V\right)\right]$ power-delay tradeoff [16]. Furthermore, by absorbing $2\tau B$ into the control parameter V, we arrive at the exact form of (17). Lemma 1 is thus proved.

REFERENCES

[1] D. Astély, E. Dahlman, A. Furuskar, Y. Jading, M. Lindstrom, and S. Parkvall, "LTE: The evolution of mobile broadband," *IEEE Commun. Mag.*, vol. 47, pp. 44–51, April 2009.

[2] D. Lee, H. Seo, B. Clerckx, E. Hardouin, D. Mazzarese, S. Nagata, and K. Sayana, "Coordinated multipoint transmission and reception in LTE-Advanced: deployment scenarios and operational challenges," *IEEE Commun. Mag.*, vol. 50, pp. 148–155, February 2012.

[3] China Mobile Research Institute, "C-RAN: The Road Towards Green RAN," *White Paper*, Sept. 2013.

[4] D. Pompili, A. Hajisami, and T. X. Tran, "Elastic resource utilization framework for high capacity and energy efficiency in cloud RAN," *IEEE Commun. Mag.*, vol. 54, no. 1, pp. 26–32, 2016.

[5] S. Bhaumik, S. P. Chandrabose, M. K. Jataprolu, G. Kumar, A. Muralidhar, P. Polakos, V. Srinivasan, and T. Woo, "Cloudiq: a framework for processing base stations in a data center," in *Proc. ACM Mobicom*, pp. 125–136, 2012.

[6] M. Madhavan, P. Gupta, and M. Chetlur, "Quantifying multiplexing gains in a wireless network cloud," in *Proc. IEEE ICC*, pp. 3212–3216, 2012.

[7] Y. Shi, J. Zhang, and K. Letaief, "Group sparse beamforming for green Cloud-RAN," *IEEE Trans. on Wireless Commun.*, vol. 13, no. 5, pp. 2809–2823, 2014.

[8] S. Luo, R. Zhang, and T. J. Lim, "Downlink and Uplink Energy Minimization Through User Association and Beamforming in C-RAN," *IEEE Trans. on Wireless Commun.*, vol. 14, no. 1, pp. 494–508, 2015.

[9] B. Dai and W. Yu, "Sparse beamforming and user-centric clustering for downlink Cloud Radio Access Network," *IEEE Access*, vol. 2, pp. 1326–1339, 2014.

[10] Y. Du and G. de Veciana, ""Wireless networks without edges": Dynamic radio resource clustering and user scheduling," in *Proc. IEEE INFOCOM*, pp. 1321–1329, 2014.

[11] T. X. Tran and D. Pompili, "Dynamic Radio Cooperation for Downlink Cloud-RANs with Computing Resource Sharing," in *Proc. IEEE MASS*, pp. 118–126, 2015.

[12] Y. Cui, Q. Huang, and V. K. Lau, "Queue-aware dynamic clustering and power allocation for network MIMO systems via distributed stochastic learning," *IEEE Trans. Signal Process.*, vol. 59, no. 3, pp. 1229–1238, 2011.

[13] H. Ju, B. Liang, J. Li, and X. Yang, "Dynamic joint resource optimization for LTE-Advanced relay networks," *IEEE Trans. on Wireless Commun.*, vol. 12, no. 11, pp. 5668–5678, 2013.

[14] P. Kyritsi, R. A. Valenzuela, and D. C. Cox, "Channel and capacity estimation errors," *IEEE Commun. Letters*, vol. 6, no. 12, pp. 517–519, 2002.

[15] W.-C. Li, T.-H. Chang, C. Lin, and C.-Y. Chi, "A convex approximation approach to weighted sum rate maximization of multiuser MISO interference channel under outage constraints," in *Proc. IEEE ICASSP*, pp. 3368–3371, 2011.

[16] M. J. Neely, "Energy optimal control for time-varying wireless networks," *IEEE Trans. Inform. Theory*, vol. 52, no. 7, pp. 2915–2934, 2006.

[17] Y. Cui, V. K. Lau, R. Wang, H. Huang, and S. Zhang, "A survey on delay-aware resource control for wireless systemslarge deviation theory, stochastic lyapunov drift, and distributed stochastic learning," *IEEE Trans. Inform. Theory*, vol. 58, no. 3, pp. 1677–1701, 2012.

[18] L. Tassiulas and A. Ephremides, "Stability properties of constrained queueing systems and scheduling policies for maximum throughput in multihop radio networks," *IEEE Trans. Autom. Control*, vol. 37, no. 12, pp. 1936–1948, 1992.

[19] L. Georgiadis, M. J. Neely, and L. Tassiulas, *Resource allocation and cross layer control in wireless networks*. Now Publishers Inc, 2006.

[20] G. Dimić and N. D. Sidiropoulos, "On downlink beamforming with greedy user selection: performance analysis and a simple new algorithm," *IEEE Trans. Signal Process.*, vol. 53, no. 10, pp. 3857–3868, 2005.

[21] V. K. Lau, F. Zhang, and Y. Cui, "Low complexity delay-constrained beamforming for multi-user MIMO systems with imperfect CSIT," *IEEE Trans. Signal Process.*, vol. 61, no. 16, pp. 4090–4099, 2013.

[22] J. Gong, S. Zhou, Z. Niu, L. Geng, and M. Zheng, "Joint scheduling and dynamic clustering in downlink cellular networks," in *Proc. IEEE GLOBECOM*, pp. 1–5, 2011.

[23] I. Bechar, "A Bernstein-type inequality for stochastic processes of quadratic forms of Gaussian variables," *arXiv preprint arXiv:0909.3595*, 2009.

[24] Z.-Q. Luo, W.-K. Ma, A.-C. So, Y. Ye, and S. Zhang, "Semidefinite relaxation of quadratic optimization problems," *IEEE Signal Process. Mag.*, vol. 27, no. 3, pp. 20–34, 2010.

[25] S. Boyd and A. Mutapcic, "Subgradient methods," *Lecture notes of EE364b, Stanford University, Winter Quarter*, vol. 2007, 2006.

[26] S. Boyd and L. Vandenberghe, *Convex optimization*. Cambridge university press, 2004.

[27] P. Baracca, F. Boccardi, and V. Braun, "A dynamic joint clustering scheduling algorithm for downlink CoMP systems with limited CSI," in *Proc. IEEE Int. Symp. on Wireless Commun. Systems (ISWCS)*, Aug. 2012.